Nonlinear Computations of Vertical Displacement Events with Toroidal Asymmetry

Carl Sovinec and Kyle Bunkers

University of Wisconsin-Madison

Theory and Simulation of Disruptions Workshop

July 17-19, 2017

Princeton Plasma Physics Lab

Outline

- Introduction -- objectives
- Modeling
- Linear stability of initial equilibria
- Nonlinear evolution
    - Development of kink instability
    - Effects from varying temperature boundary conditions
    - Assessment of simplifications
- Initialization with fitted equilibria
- Conclusions and future work

Introduction: There are at least two distinct objectives for VDE modeling.

1. Characterization of disruptive transients
   - Investigate interactions among multiple physical processes: MHD, external electromagnetics, plasma and impurity transport, plasma-surface interaction, and radiation.
   - This objective emphasizes comprehensive modeling.
2. Practical modeling for addressing specific questions
   - Assessing wall forces is an example.
   - If validated, faster reduced modeling is preferable.

Our long-term aim is the first objective, but we consider approximations that may be useful for the second.

Model: Our computations presently use visco-resistive MHD with fluid closures.

- Fluid-based models describe the evolution of low-order moments of particle distributions and low-frequency electromagnetics.

$\frac{\partial n}{\partial t} + \nabla \cdot (n\mathbf{V}) = \nabla \cdot \left(D_n \nabla n - D_h \nabla \nabla^2 n \right)$	particle continuity with artificial diffusion
$mn\left(\frac{\partial}{\partial t} + \mathbf{V} \cdot \nabla \right)\mathbf{V} = \mathbf{J} \times \mathbf{B} - \nabla(2nT) - \nabla \cdot \underline{\Pi} - \nu_n mn\mathbf{V}$	momentum density with optional drag
$\frac{n}{\gamma - 1}\left(\frac{\partial}{\partial t}T + \mathbf{V} \cdot \nabla T \right) = -nT\nabla \cdot \mathbf{V} - \nabla \cdot \mathbf{q}$	temperature evolution
$\frac{\partial \mathbf{B}}{\partial t} = -\nabla \times (\eta \mathbf{J} - \mathbf{V} \times \mathbf{B})$	Faraday's law & MHD Ohm's
$\mu_0 \mathbf{J} = \nabla \times \mathbf{B}$	Ampere's law
$\nabla \cdot \mathbf{B} = 0$	divergence constraint

- The NIMROD code (https://nimrodteam.org) is used to solve linear and nonlinear versions of this system.

Closure relations approximate transport effects.

- Normalized equations are used in this application.
  - $\tau_A \equiv R_0^2 / F_{open} \cong 1; \quad \mu_0 \to 1, \quad n_0 \to 1$
  - $a \cong 0.8; \quad R_0 = 1.6$
- Magnetic diffusivity depends on temperature.
  - $\eta_0 / \mu_0 = 1 \times 10^{-6}$
  - $\eta(T) = \min\left[\eta_0 \left(T_0 / T\right)^{3/2}, 1\right]$
- Thermal conduction and viscous stress are anisotropic with fixed coefficients.
  - $\mathbf{q} = -n\left[\left(\chi_{\|} - \chi_{iso}\right)\hat{\mathbf{b}}\hat{\mathbf{b}} + \chi_{iso}\underline{\mathbf{I}}\right] \cdot \nabla T; \quad \chi_{\|} = 7.5 \times 10^{-2}, \quad \chi_{iso} = 7.5 \times 10^{-6}$
  - $\underline{\Pi} = \nu_{\|} mn\left(\underline{\mathbf{I}} - 3\hat{\mathbf{b}}\hat{\mathbf{b}}\right)\hat{\mathbf{b}} \cdot \underline{\mathbf{W}} \cdot \hat{\mathbf{b}} - \nu_{iso} mn\underline{\mathbf{W}}; \quad \nu_{\|} = 5 \times 10^{-2}, \quad \nu_{iso} = 5 \times 10^{-5}$

    $$\underline{\mathbf{W}} = \nabla\mathbf{V} + \nabla\mathbf{V}^T - \frac{2}{3}\underline{\mathbf{I}}\nabla \cdot \mathbf{V}$$
- Artificial diffusivities are intended to be small.
  - $D_n = 5 \times 10^{-6}, \quad D_h = 1 \times 10^{-10}$

The computations presented here use the following boundary conditions.

- Normal component of flow-velocity is $\mathbf{E}_{wall} \times \mathbf{B}$ drift.
  - Choice is based on previously described axisymmetric tests.
  - $\mathbf{E}_{wall}$ is from resistive diffusion through the wall.
- Density at the wall is fixed: $n_{wall} = 0.1 n_0$
  - Diffusion allows particles to move through the wall.
- Resistive diffusion through the wall is at an intermediate time-scale.
  - $v_{wall} = \eta_0 / \mu_0 \Delta x_{wall} = 1 \times 10^{-3}$
  - An outer vacuum region is surrounded by a conducting wall.
  - Small (10^{-7}) magnetic field errors in n = 1 and n = 2 are applied in nonlinear computations.
- Most computations use a Dirichlet condition on temperature.
  - T_{wall} is fixed at a value $\leq T_0 / 10^4$ for these cases.
  - For a comparative test, one case uses insulating conditions.

Initial conditions are up-down symmetric, diverted equilibria.

- Two equilibrium states are considered.
  - Primary difference is *q*.
  - Both have $\beta_0 \cong 1\%$.

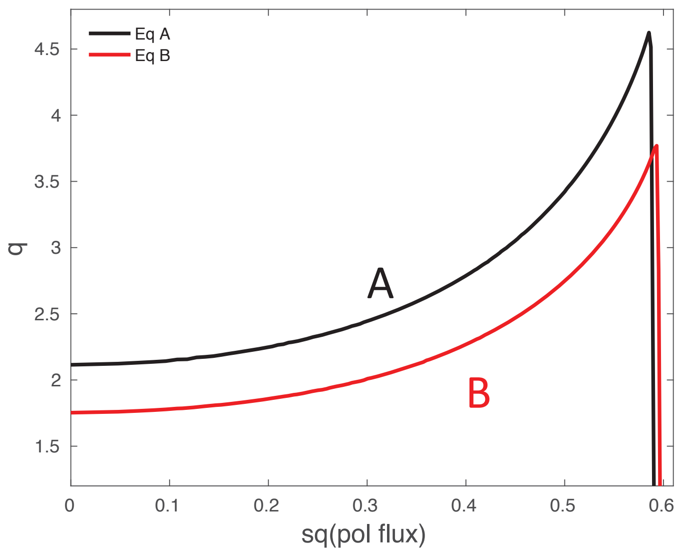

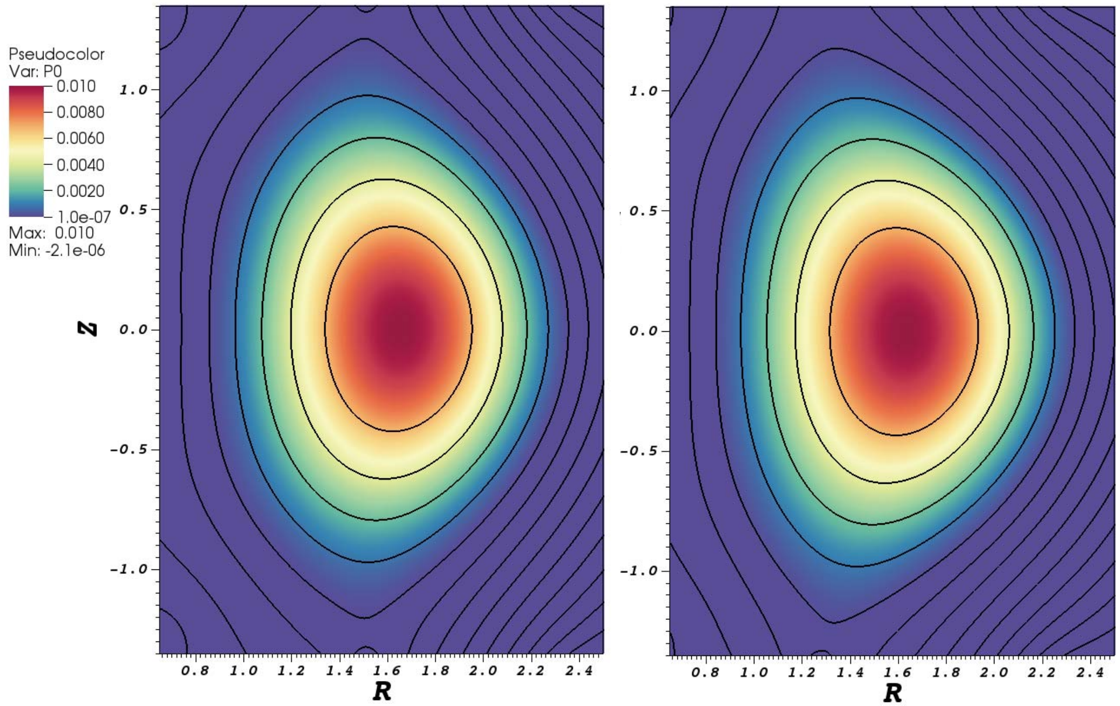

Contours of poloidal flux and pressure for Eq. A (left) and Eq. B (right).

- VDEs are initiated by removing current from the upper divertor coil (outside wall).

Linear Results: Linear computations evolve perturbations in the initial (static) equilibria.

- With the large edge resistivity and no flow, edge modes are unstable.

Growth rates computed for the initial equilibria with conducting wall.

n	$\gamma\tau_A$, Eq. A	$\gamma\tau_A$, Eq. B
1	2.5×10^{-3}	1.7×10^{-2}
2	1.4×10^{-3}	-
3	2.6×10^{-3}	1.8×10^{-3}
4	3.4×10^{-3}	-

- Low-n growth rates increase only somewhat with the resistive wall with $v_{wall} = 1\times10^{-3}$.

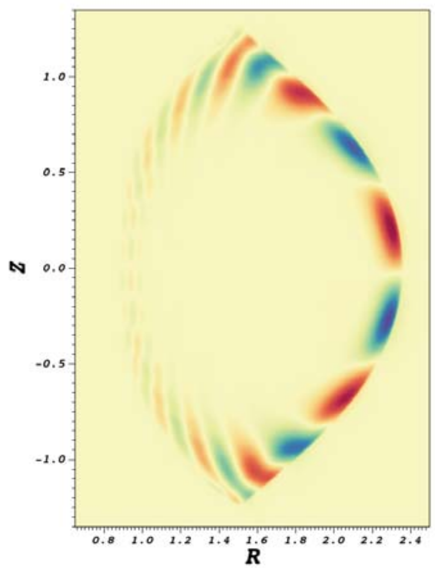

***n* = 3 mode of Eq. A has ballooning character. [Pressure is shown.]**

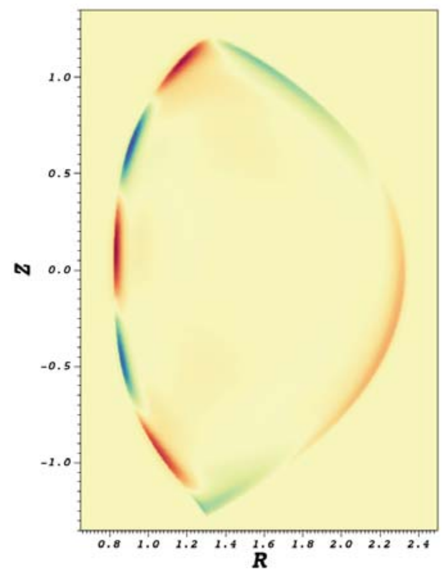

***n* = 1 mode of Eq. B is concentrated on the inboard side.**

Nonlinear Results: With vertical displacement, $n = 1$ grows faster than the linear prediction.

- For Eq. A (high-q), $n = 1$ growth rate rapidly increases to $\gamma\tau_A \cong 2.5\times10^{-2}$.

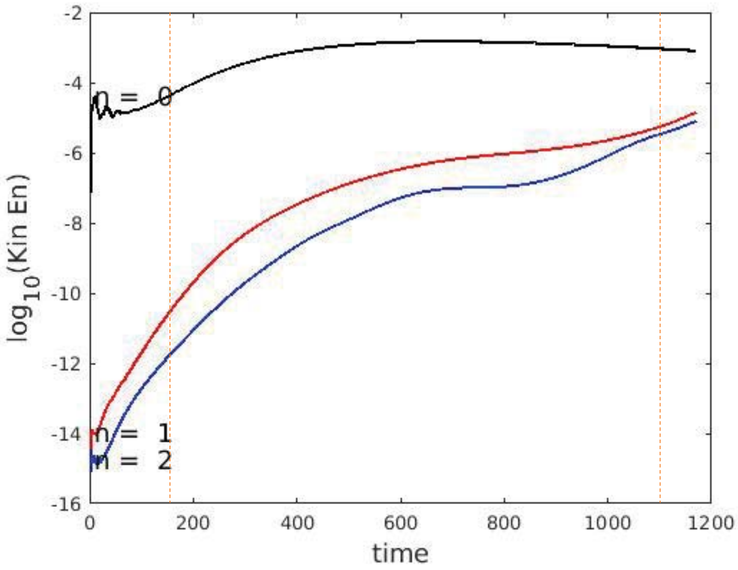

Evolution of kinetic energy fluctuations from low resolution (0≤*n*≤2) case starting from Eq. A.

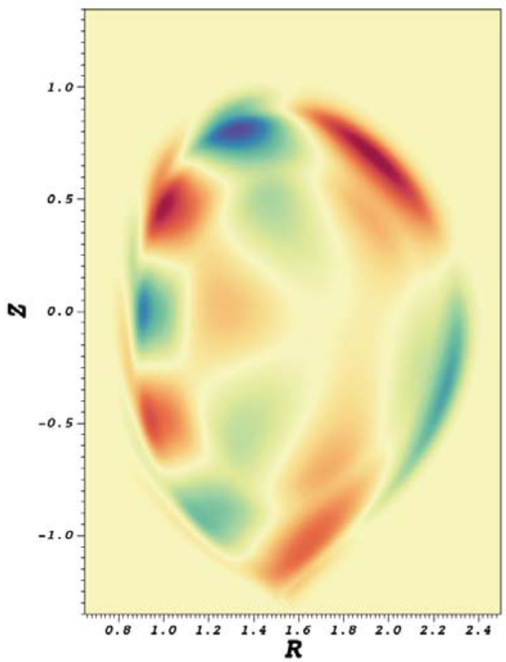

***n* = 1 pressure contours at *t* = 160 primarily shows *m* = 4.**

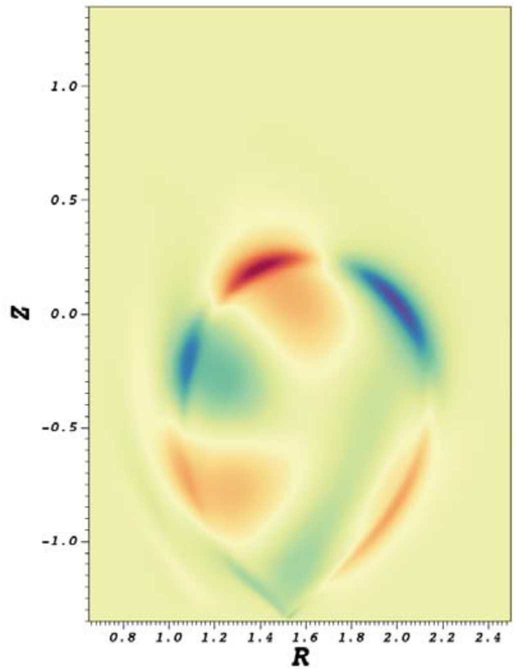

At *t* = 1110, the mode is *m* = 3.

Robust instability is a consequence of edge profile changes from wall contact.

- Loss of edge RB_ϕ and pressure enhances edge current.
- The (3,1) mode develops while the (4,1) is suppressed with decreasing $q(a)$.

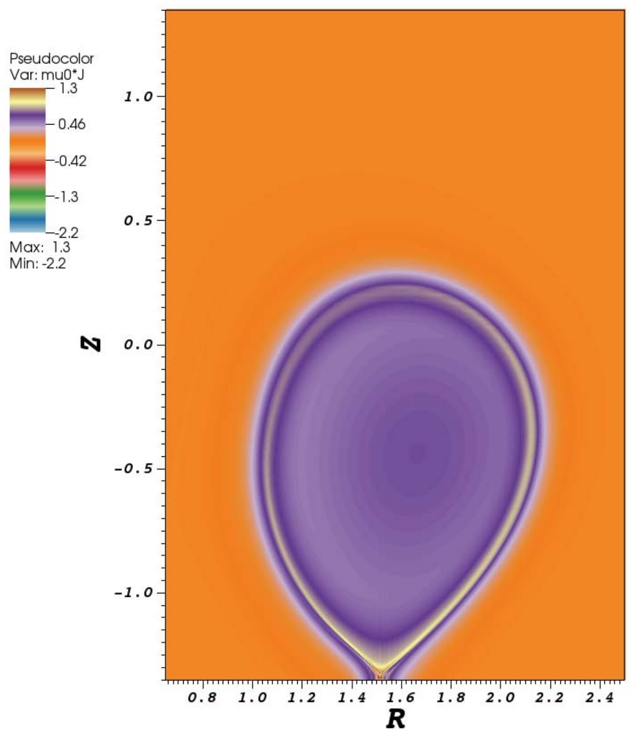

A strong current layer develops at the edge of the closed flux. [Plot shows $\langle\lambda\rangle = \langle\mu_0 J.B/B^2\rangle$ at t = 1110.]

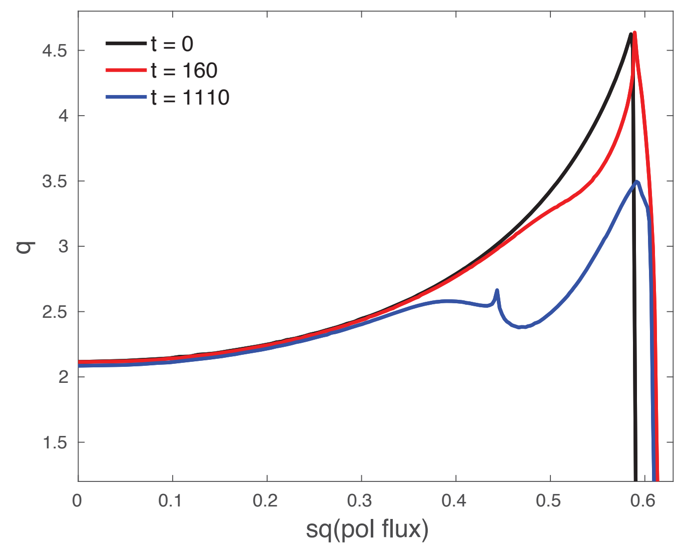

With increasing displacement, edge q is reduced, and edge-$\langle\lambda\rangle$ creates reversed shear.

Similar evolution occurs with increased toroidal resolution.

- Another computation adds Fourier components 3≤*n*≤5 to the previous Eq.-A computation at *t* = 740.
- The evolution of low-*n* components is not altered appreciably.
- Both computations eventually terminate due to inadequate resolution.

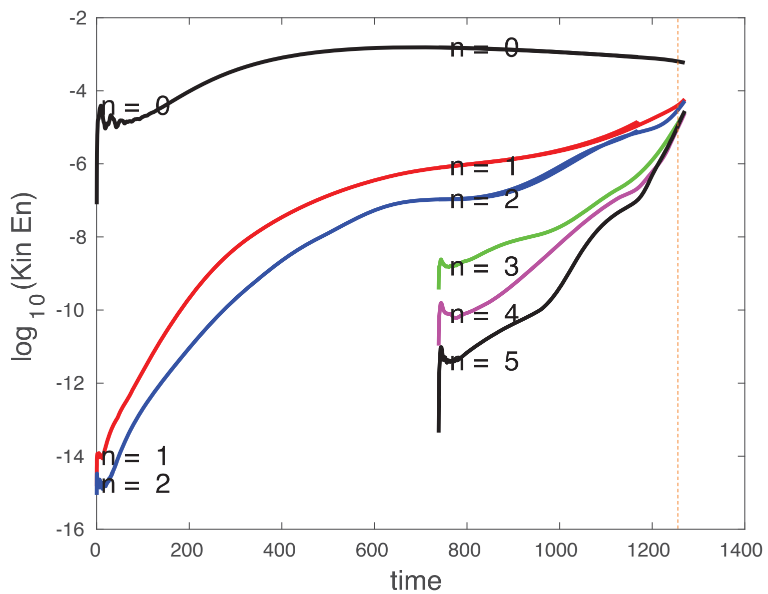

Overlay of kinetic fluctuation energies from the two Eq.-A computations.

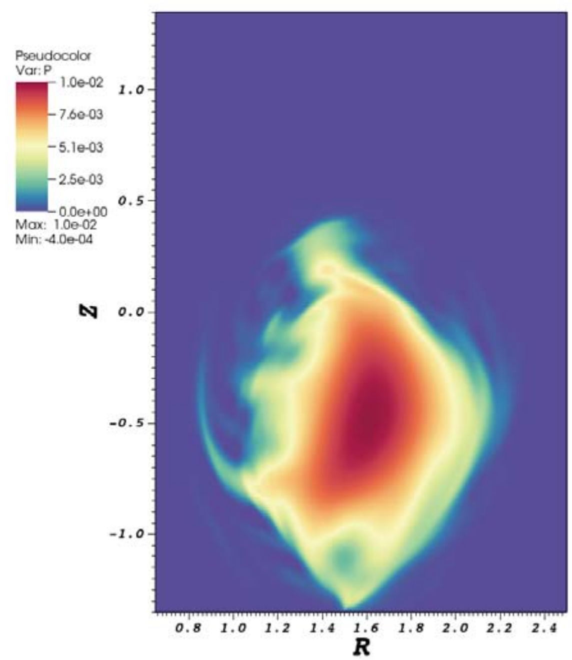

Contours of pressure at $\phi = 0$, *t*=1260 indicate 3D distortion.

Nonlinear evolution from Eq. B (lower *q*) is faster.

- A higher-resolution Eq.-B computation uses 0≤*n*≤10 from the start.
- Transition from (4,1) to (3,1) occurs without hesitation.

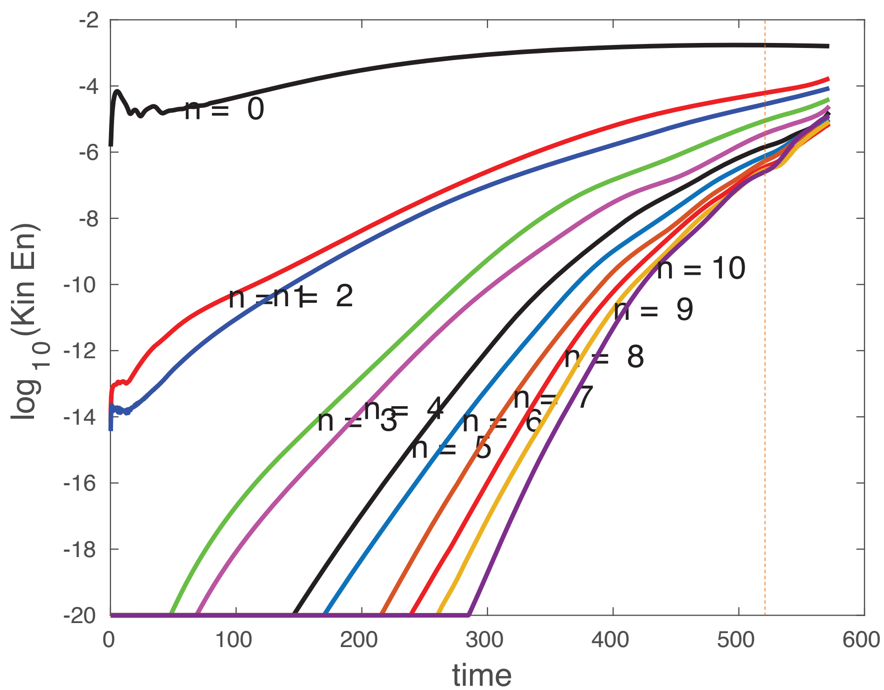

Evolution of kinetic fluctuation energies shows robust growth throughout.

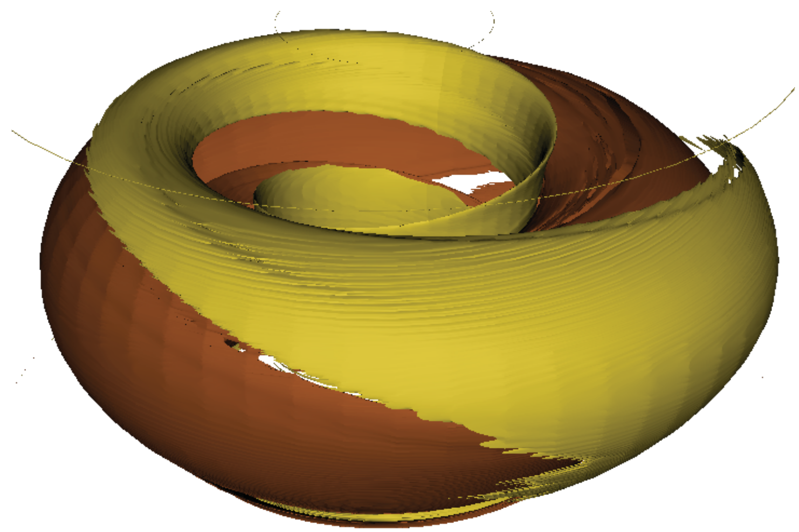

Isosurfaces of λ = -0.085 (mustard) and λ = +0.8 (brown) at *t* = 519. The negative region opposes the direction of plasma current.

The mode imposes toroidal variation in the conductive current density along the 'divertor' surface.

- The results show $O(1)$ toroidal variation in the surface-normal component of current density.
- The spatial variation is primarily $n = 1$, but larger-n harmonics are also evident.

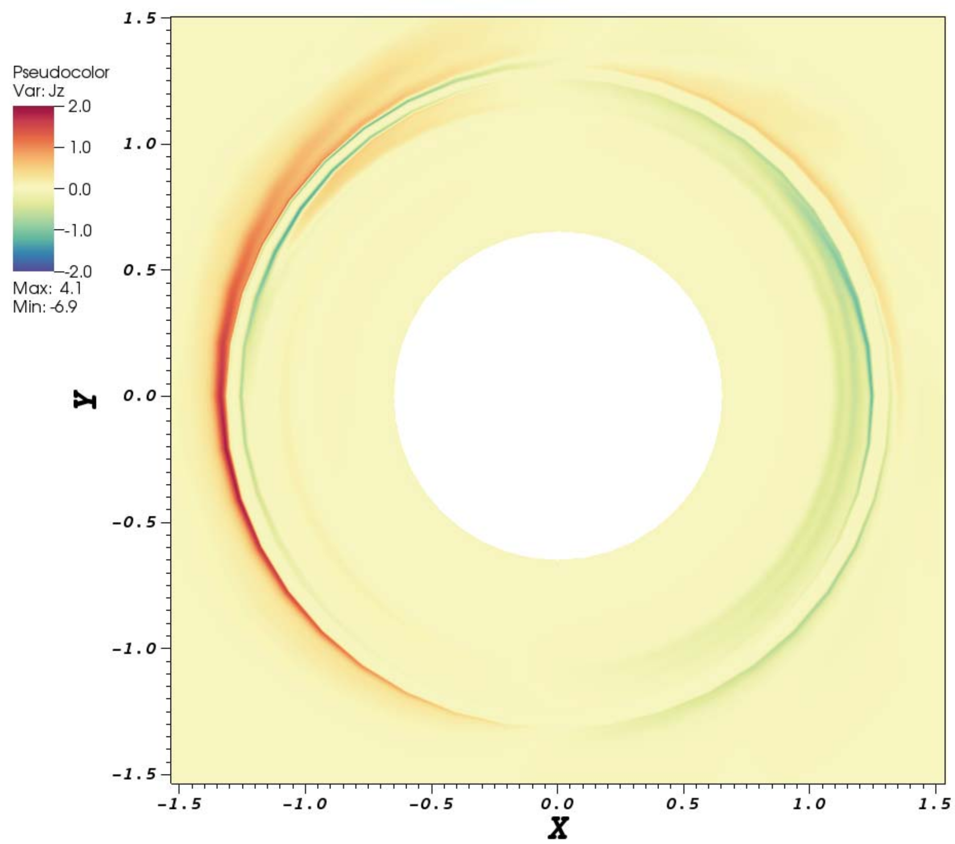

Contours of J_z just above the lower surface at t = 519.

Through the early phases, evolution of global parameters is similar to axisymmetric results.

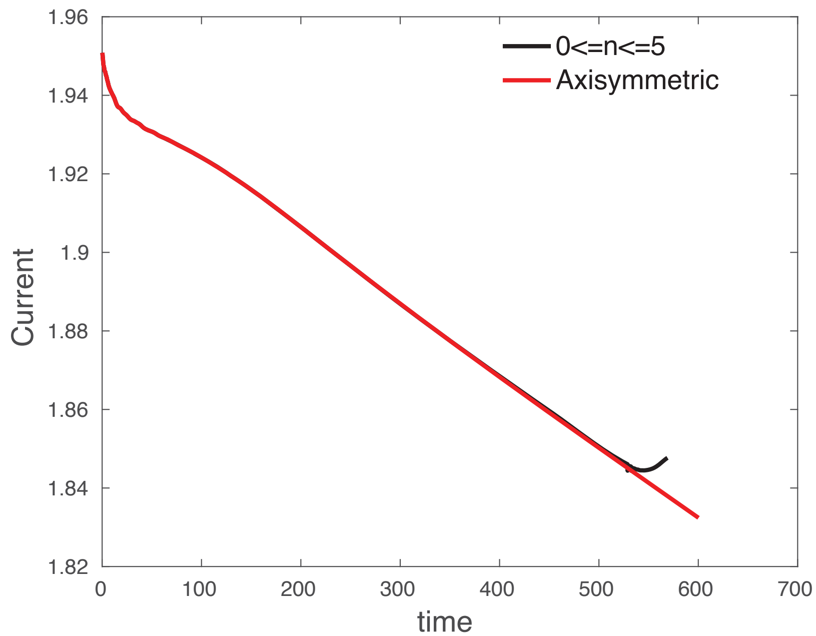

Evolution of plasma current for 3D and axisymmetric Eq.-B computations.

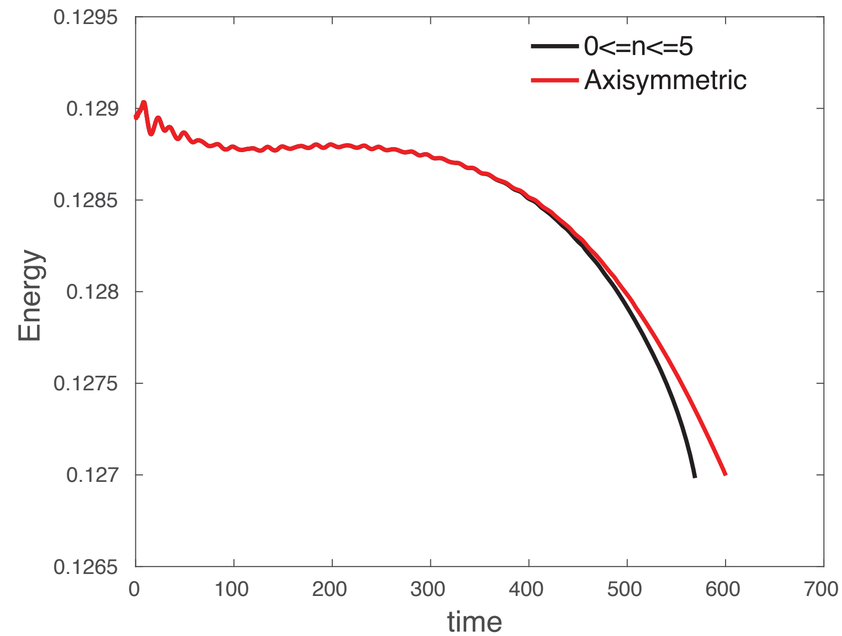

Evolution of thermal energy for the two computations.

- Seemingly significant distortions of the pedestal-region plasma are slow to impact overall evolution.
- This is also true for Eq.-A computations.

Assessment of simplifications: Several simplifications have been considered.

1. Reduced resolution of toroidal coordinate
   - Limit Fourier expansion and/or use filtering.
   - ➢ The highly nonlinear phase needs fine resolution.
2. Using the drag term to limit the range of dynamics
   - This is analogous to tokamak-MHD.
   - ➢ The peeling modes observed here grow too quickly.
3. Approximating $n(\mathbf{x},t)$ as <$n(\mathbf{x},t)$> in dissipation coefficients and inertia
   - $\langle n \rangle \equiv \int_0^{2\pi} n\, d\phi \big/ 2\pi$
   - $n(\mathbf{x},t)$ is always evolved in 3D for pressure, $n(\mathbf{x},t)T(\mathbf{x},t)$.
   - Other nonlinearities are simplified with <$n(\mathbf{x},t)$>.
   - ➢ Artificial energy loss/gain may occur.

Axisymmetric computations from Eq. A indicate sensitivity to heat flux modeling at the wall.

- The computation with Dirichlet conditions on T loses approximately 20% of its thermal energy over the first 1400 τ_A .
- The insulating condition slows the evolution of I_p.

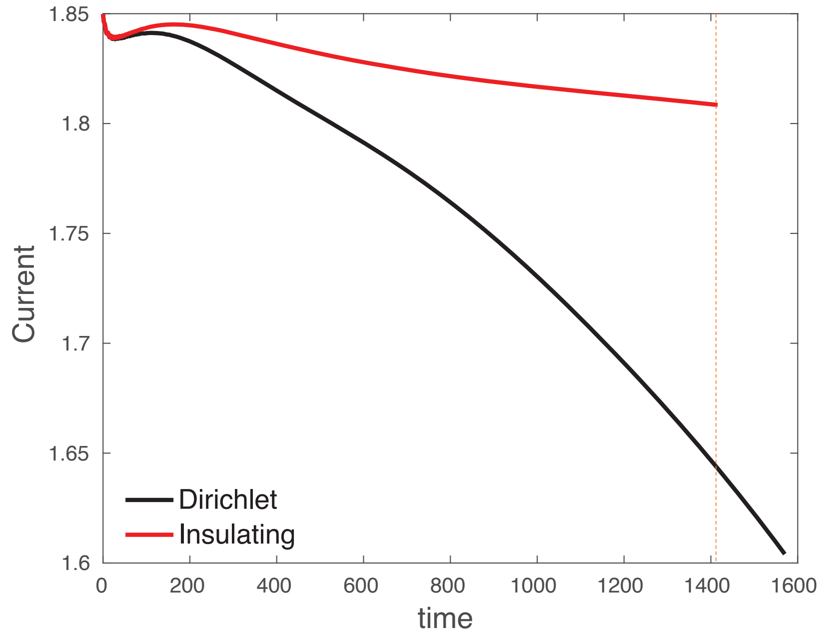

Evolution of plasma current is sensitive to boundary conditions on *T*.

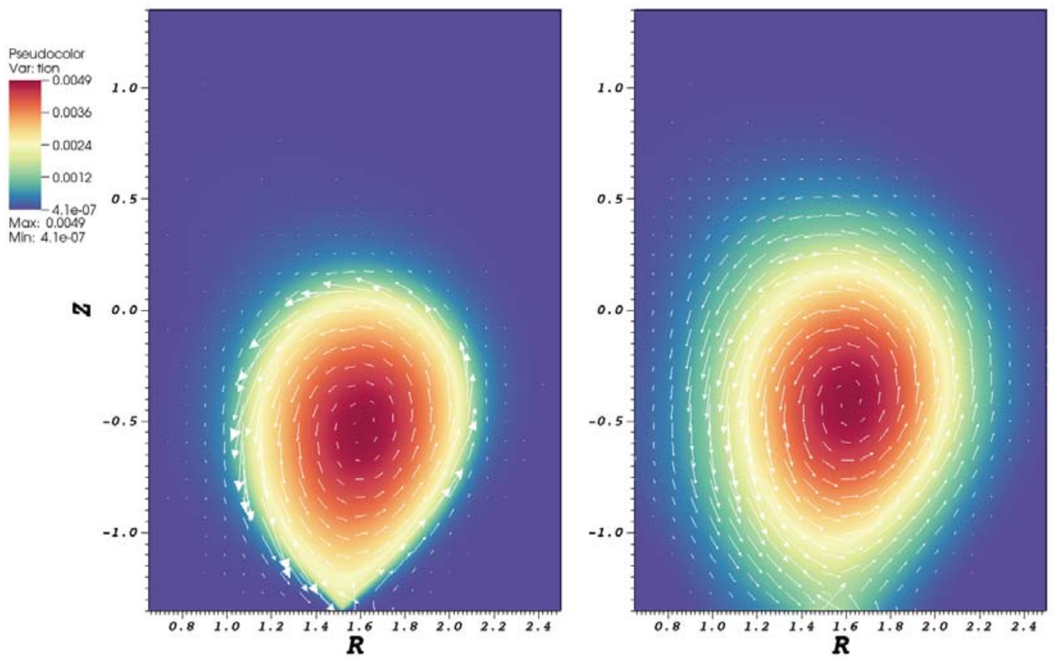

Contours of *T* with J vectors overlaid at *t* = 1410 with Dirichlet (left) and insulating (right).

Initialization from fitted equilibria: We have developed a new procedure for our VDE computations.

- Equilibria for VDE computations with resistive walls need consistent flux values from external coils and internal currents.
- We now use EFIT data for the plasma current density.
- Wall flux in fixed-boundary solves is from coil currents and the plasma current.
- NIMEQ [Howell, CPC **185**, 1415] is used to generate the equilibrium on the NIMROD VDE mesh.

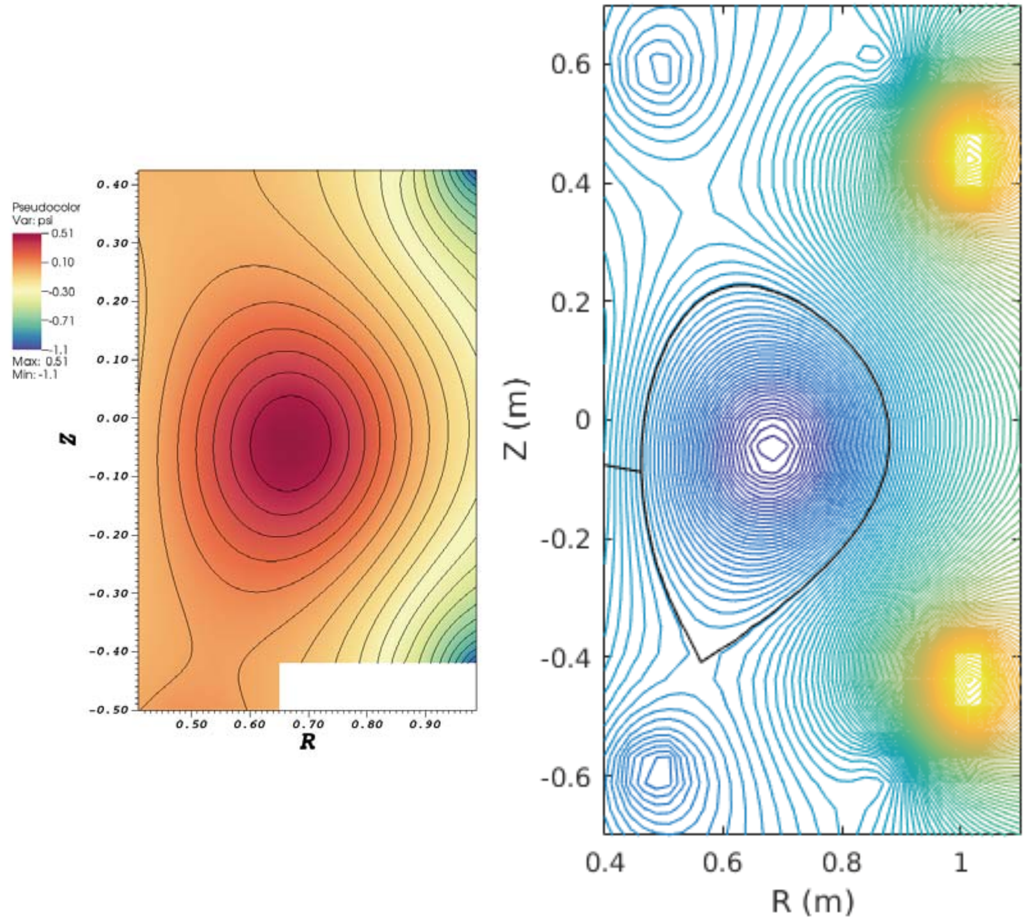

Recomputed equilibrium for NIMROD (left) and EFIT of C-MOD 1160511013 (right), courtesy of Alex Tinguely.

Conclusions

- Our 3D computations point to edge peeling/kink.
  - In addition to open-field halo, a strong edge current develops for force balance.
  - This current layer destabilizes the edge region.
- The comparison of axisymmetric results emphasizes edge and plasma-surface modeling.
  - Dirichlet and insulating conditions represent limits.
  - More detailed modeling is needed.
- Simplifications have limited benefit for this type of modeling.